Emergent Sp(3,ℝ) Dynamical Symmetry in the Nuclear Many-Body System from an *Ab Initio* Description

Anna E. McCoy,[1,2] Mark A. Caprio,[2] Tomáš Dytrych,[3,4] and Patrick J. Fasano[2]
[1]*TRIUMF, Vancouver, British Columbia V6T 2A3, Canada*
[2]*Department of Physics, University of Notre Dame, Notre Dame, Indiana 46556, USA*
[3]*Nuclear Physics Institute, Academy of Sciences of the Czech Republic, 250 68 Řež, Czech Republic*
[4]*Department of Physics and Astronomy, Louisiana State University, Baton Rouge, Louisiana 70803, USA*

(Received 5 October 2019; accepted 10 August 2020; published 3 September 2020)

Ab initio nuclear theory provides not only a microscopic framework for quantitative description of the nuclear many-body system, but also a foundation for deeper understanding of emergent collective correlations. A symplectic $\mathrm{Sp}(3,\mathbb{R}) \supset \mathrm{U}(3)$ dynamical symmetry is identified in *ab initio* predictions, from a no-core configuration interaction approach, and found to provide a qualitative understanding of the spectrum of ^{7}Be. Low-lying states form an Elliott SU(3) spectrum, while an $\mathrm{Sp}(3,\mathbb{R})$ excitation gives rise to an excited rotational band with strong quadrupole connections to the ground state band.

DOI: 10.1103/PhysRevLett.125.102505

The nucleus is a complex many-body system, which nonetheless exhibits simple patterns indicative of emergent collective degrees of freedom [1–4]. *Ab initio* nuclear theory now provides accurate quantitative predictions for observables in light nuclei [5–14]. Signatures of collective phenomena including clustering [14–19] and rotation [12,20–23] emerge from *ab initio* calculations. This leaves us with the question of understanding the underlying physical nature of the collective correlations giving rise to these patterns.

In a system exhibiting dynamical symmetry [24–28], simple patterns arise naturally, since the spectrum of eigenstates is organized according to irreducible representations (*irreps*) of the dynamical symmetry group. In heavier nuclei, dynamical symmetries have played a central role in characterizing nuclear correlations and collective phenomena [29,30]. In intermediate-mass nuclei, described by the shell model, Elliott's SU(3) dynamical symmetry [31–33] provides a mechanism for the emergence of rotation. In the lightest nuclei, accessible by *ab initio* theory, we may now seek to identify the role of $\mathrm{Sp}(3,\mathbb{R}) \supset \mathrm{U}(3)$ dynamical symmetry [34–36] in defining the structure of the excitation spectrum.

The symplectic group $\mathrm{Sp}(3,\mathbb{R})$, associated with the coordinates and momenta in three dimensions, has long been proposed as an organizing scheme for the nuclear many-body problem [34–37]. Through its U(3) subgroup, the symmetry group of the harmonic oscillator, it is intimately connected to the nuclear shell model [34,35,38–44]. In its contraction limit, $\mathrm{Sp}(3,\mathbb{R})$ yields a microscopic formulation of nuclear collective dynamics, in terms of coupled rotational and giant monopole and quadrupole vibrational degrees of freedom [45,46].

Wave functions obtained in *ab initio* calculations have already been identified as having specific dominant U(3) and $\mathrm{Sp}(3,\mathbb{R})$ symmetry components [9,47–54]. In this Letter, calculations carried out in a symplectic no-core configuration interaction (SpNCCI) framework demonstrate that the symmetry of individual states moreover fits into an overall $\mathrm{Sp}(3,\mathbb{R}) \supset \mathrm{U}(3)$ dynamical symmetry pattern of the spectrum as a whole.

In particular, for ^{7}Be, beyond the well-known $K = 1/2$ ground state rotational band [20–22], we find that an excited band emerges in the *ab initio* calculations as a symplectic collective excitation. The remainder of the low-lying spectrum follows an Elliott SU(3) dynamical symmetry pattern, where the rotational structure is, however, dressed by multishell symplectic excitations. Preliminary results were presented in Refs. [55,56].

$\mathrm{Sp}(3,\mathbb{R}) \supset \mathrm{U}(3)$ *dynamical symmetry.*—To recognize the role of $\mathrm{Sp}(3,\mathbb{R}) \supset \mathrm{U}(3)$ dynamical symmetry in *ab initio* calculated spectra, we must first be familiar with some basic properties of $\mathrm{Sp}(3,\mathbb{R})$ irreps. Elliott's $\mathrm{U}(3) = \mathrm{U}(1) \times \mathrm{SU}(3)$ group considered here is the product of an SU(3) generated by the orbital angular momentum operator and a quadrupole tensor $\mathcal{Q}$, and the U(1) group of the harmonic oscillator Hamiltonian. Then $\mathrm{Sp}(3,\mathbb{R})$ augments these generators with symplectic raising and lowering operators, which physically represent creation and annihilation operators for giant monopole and quadrupole vibrations.

An $\mathrm{Sp}(3,\mathbb{R})$ irrep is comprised of an infinite tower of U(3) irreps. Starting from a single U(3) irrep with some lowest number of oscillator quanta, or *lowest grade irrep* (LGI), the remaining U(3) irreps are obtained by repeatedly acting with the symplectic raising operator, which adds two oscillator quanta at a time. Each U(3) irrep is characterized by a fixed number of oscillator quanta and by SU(3) quantum numbers (λ,μ), which are related to the nuclear deformation [57]. A U(3) irrep may therefore be labeled by

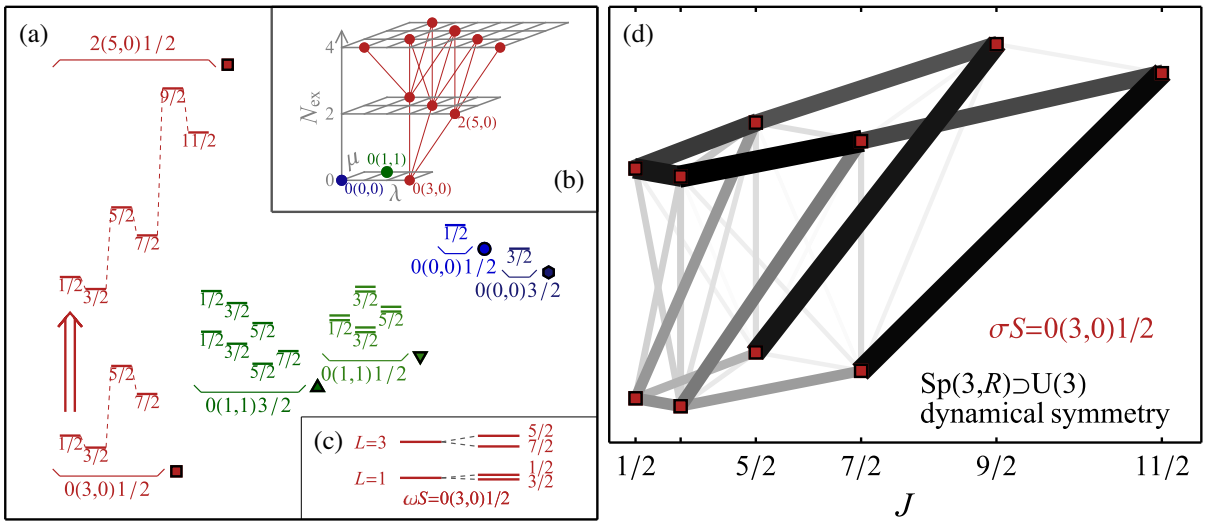

FIG. 1. Low-lying spectrum in an $\mathrm{Sp}(3,\mathbb{R}) \supset \mathrm{U}(3)$ dynamical symmetry description of ^{7}Be. (a) Energies. Parameters in the dynamical symmetry Hamiltonian (2) are chosen for approximate consistency with the experimental [58] and *ab initio* calculated spectra of ^{7}Be. States are grouped by U(3) irreps (labeled by ωS). The excited $\omega S = 2(5,0)1/2$ U(3) irrep obtained by symplectic raising (arrow) within the $\sigma S = 0(3,0)1/2$ $\mathrm{Sp}(3,\mathbb{R})$ irrep is shown. To facilitate comparison with Fig. 2, $\mathrm{Sp}(3,\mathbb{R})$ irreps are tagged by symbols defined there for σS. (b) Organization of $\mathrm{Sp}(3,\mathbb{R})$ irrep $\sigma = 0(3,0)$ into U(3) irreps (dots), connected by the symplectic raising operator (lines). Shown through $N_{\mathrm{ex}} = 4$. (c) Branching of the U(3) irrep 0(3,0) to orbital angular momenta L, followed by coupling with spin ($S = 1/2$) to give total angular momenta J. (d) Quadrupole transition strengths (isoscalar), within the $\sigma S = 0(3,0)1/2$ $\mathrm{Sp}(3,\mathbb{R})$ irrep, with $B(E2)$ strength indicated by line thickness (and shading).

quantum numbers $\omega \equiv N_{\omega,\mathrm{ex}}(\lambda_\omega,\mu_\omega)$, where N_{ex} denotes the number of oscillator excitations relative to the lowest Pauli-allowed oscillator configuration. The entire $\mathrm{Sp}(3,\mathbb{R})$ irrep is then uniquely labeled by the U(3) quantum numbers $\sigma \equiv N_{\sigma,\mathrm{ex}}(\lambda_\sigma,\mu_\sigma)$ of its LGI. The $2\hbar\omega$ and $4\hbar\omega$ U(3) irreps arising through the action of the symplectic raising operator on the $\sigma = 0(3,0)$ LGI in ^{7}Be are illustrated in Fig. 1(b).

The full subgroup chain, taking into account angular momenta, is

$$[\underbrace{\mathrm{Sp}(3,\mathbb{R})}_{\sigma} \supset \underbrace{\mathrm{U}(3)}_{\omega} \supset \mathrm{SO}(3)_L] \times \mathrm{SU}_S(2) \supset \mathrm{SU}_J(2). \quad (1)$$

Each U(3) irrep contains states of orbital angular momenta L according to the $\mathrm{SU}(3) \supset \mathrm{SO}(3)$ branching rule [31]. Fermionic antisymmetry defines the possible total spins S [32,59,60] for each U(3) irrep realized in the nuclear many-body system. Then L and S combine to give total angular momenta J, as illustrated in Fig. 1(c) for the $\omega = 0(3,0)$ irrep in ^{7}Be, where $L = 1, 3$ combine with $S = 1/2$ to give $J = 1/2, 3/2, 5/2, 7/2$.

The low-energy spectrum expected in a dynamical symmetry description of ^{7}Be is illustrated in Fig. 1(a). In the $0\hbar\omega$ (or valence) space, the U(3) irreps which arise have $\omega = 0(3,0)$, 0(1,1) and 0(0,0), appearing in combination with specific spins S as shown in Fig. 1(a). Each serves as the LGI of an $\mathrm{Sp}(3,\mathbb{R})$ irrep (with $N_{\sigma,\mathrm{ex}} = 0$). The U(3) irrep with $\omega S = 2(5,0)1/2$ obtained by symplectic laddering from the $\sigma S = 0(3,0)1/2$ LGI is shown. Then, further $\mathrm{Sp}(3,\mathbb{R})$ irreps originate at higher $N_{\sigma,\mathrm{ex}}$.

The energy spectrum in Fig. 1 is determined by a simple dynamical symmetry Hamiltonian constructed from the Casimir operators for the subgroup chain (1):

$$H = \alpha C_{\mathrm{Sp}(3,\mathbb{R})} + \varepsilon H_0 + \beta C_{\mathrm{SU}(3)} + a_L \mathbf{L}^2 + a_S \mathbf{S}^2 + \xi \mathbf{L}\cdot\mathbf{S}. \quad (2)$$

Here, $C_{\mathrm{Sp}(3,\mathbb{R})}$ is the Casimir operator of $\mathrm{Sp}(3,\mathbb{R})$ [44], while the SU(3) Casimir operator $C_{\mathrm{SU}(3)} = (1/6)(\mathcal{Q}\cdot\mathcal{Q} + 3\mathbf{L}^2)$ incorporates the classic Elliott quadrupole Hamiltonian [32]. The $\mathbf{J}^2$ angular momentum Casimir operator is absorbed into $\mathbf{L}\cdot\mathbf{S} = \frac{1}{2}(\mathbf{J}^2 - \mathbf{L}^2 - \mathbf{S}^2)$.

A $K = 1/2$ ground-state band is experimentally observed in ^{7}Be (and mirror nuclide ^{7}Li) [58,61], with an exaggerated Coriolis energy staggering leading to an inverted angular momentum sequence ($J = 3/2, 1/2, 7/2, 5/2$). When the usual attractive sign is taken on the quadrupole interaction in Eq. (2), i.e., $\beta < 0$, the leading (lowest energy) U(3) irrep is 0(3,0), which indeed has the same angular momentum content [Fig. 1(c)] as the ^{7}Be ground-state band. The staggering is qualitatively reproduced via the $\mathbf{L}\cdot\mathbf{S}$ dependence in Eq. (2).

Dynamical symmetry provides concrete predictions also for transition strengths [27,28]. The isoscalar part of the quadrupole operator is a linear combination of $\mathrm{Sp}(3,\mathbb{R})$

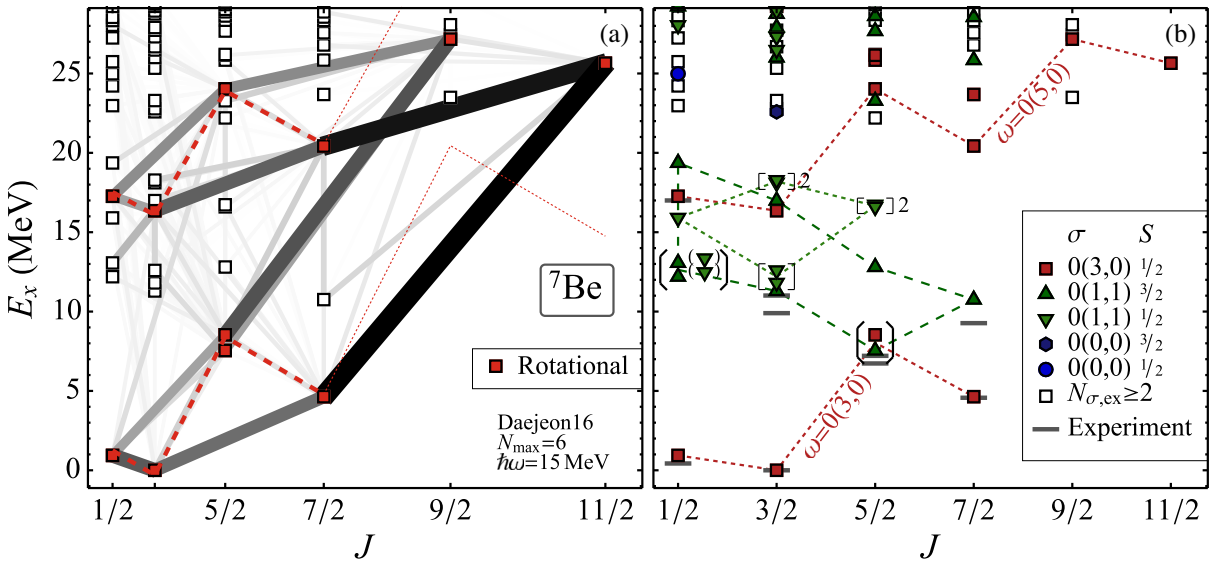

FIG. 2. *Ab initio* calculated negative parity energy spectrum of ^{7}Be: (a) Rotational bands (red squares). Strengths (line thickness and shading) are indicated for all J-decreasing $E2$ transitions from rotational band members (specifically, $J_f < J_i$ or $J_f = J_i$ and $E_f < E_i$). Energies are plotted against angular momentum scaled as $J(J+1)$, as appropriate for rotational analysis. Fits to the rotational energy formula with Coriolis staggering are shown (dashed or dotted lines). (b) Most significant $\mathrm{Sp}(3,\mathbb{R})$ contribution σS (indicated by symbol shape and color, see legend) for each state. States with the same largest U(3) contribution ωS are connected by dashed lines. Close-lying states may represent degenerate subspaces involving different internal spin couplings (square brackets, with a numeral 2 indicating degenerate doublets indistinguishable in the plot) or may undergo significant two-state mixing (angled brackets). Experimental energies [58] are shown for context (horizontal lines). Calculation is for the Daejeon16 interaction, with $N_{\max} = 6$ and oscillator basis parameter $\hbar\omega = 15$ MeV [71].

generators. Thus, $\mathrm{Sp}(3,\mathbb{R}) \supset \mathrm{U}(3)$ dynamical symmetry implies strong $E2$ transitions between U(3) irreps differing by two quanta within an $\mathrm{Sp}(3,\mathbb{R})$ irrep. Predictions for isoscalar $E2$ strengths follow directly from $\mathrm{Sp}(3,\mathbb{R})$ generator matrix elements [62,63], with no free parameters, as illustrated in Fig. 1(d) for $\sigma S = 0(3,0)1/2$.

Ab initio SpNCCI results for ^{7}Be.—The present SpNCCI framework for *ab initio* calculations makes use of a symmetry-adapted basis for the fermionic many-body space, one which reduces the subgroup chain (1) and is free of center-of-mass excitations. Matrix elements of the Hamiltonian and other operators are obtained recursively in terms of matrix elements between the LGIs, building on the ideas of Reske, Suzuki, and Hecht [64–66]. These seed matrix elements are calculated using the U(3)-coupled symmetry-adapted no-core shell model (SA-NCSM) [9,52]. Details may be found in Ref. [56].

Here we carry out SpNCCI calculations for ^{7}Be with the Daejeon16 internucleon interaction [67], in a basis incorporating all $\mathrm{Sp}(3,\mathbb{R})$ irreps with LGIs with up to 6 quanta ($N_{\sigma,\mathrm{ex}} \leq 6$), and carrying each of these up to 6 quanta ($N_{\omega,\mathrm{ex}} \leq 6$), both taken relative to the lowest Pauli-allowed configuration. The resulting space is simply the center-of-mass free subspace [68,69] of the $N_{\max} = 6$ no-core shell model (NCSM) space [70], and the spectroscopic results, shown in Fig. 2(a), are identical to those of a traditional $N_{\max} = 6$ calculation.

Although symmetry-adapted bases combined with physically motivated truncation schemes can yield improved convergence of calculations [49,52], our interest here lies in understanding how the dynamical symmetry structure of ^{7}Be underlies the features of the *ab initio* calculated spectrum. Since the basis reduces the subgroup chain (1), SpNCCI calculations provide immediate access to the $\mathrm{Sp}(3,\mathbb{R})$ and U(3) symmetry decompositions of the calculated wave functions, as illustrated in Fig. 3. Further decompositions are provided in the Supplemental Material [72].

Notably, rotational features emerge in the spectrum. A $K = 1/2$ ground state band ($J = 1/2$ through $7/2$) is readily recognized through enhanced $E2$ transitions in the *ab initio* calculated spectrum [Fig. 2(a), lower dashed line], as in earlier NCSM calculations [20–22]. Calculated excitation energies within the band are already largely insensitive to $N_{\max}$ even though absolute energies are not well converged (see Ref. [73]).

Moreover, two higher angular momentum states ($9/2^-_2$ and $11/2^-_1$) have strong $E2$ connections to this ground state band. In previous NCSM calculations [20–22], these states have been considered as possible ground state band members, albeit with energies above those expected from the standard rotational energy formula with Coriolis staggering [Fig. 2(a), lower dotted line]. Their quadrupole moments are also anomalously large compared to the ground state band members (Fig. 5 of Ref. [21]).

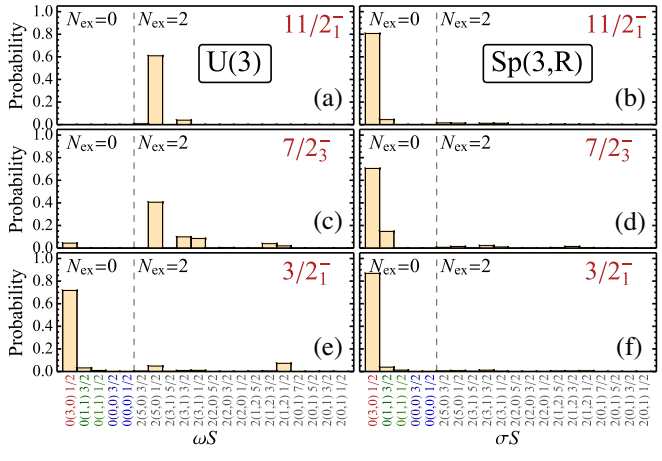

FIG. 3. Decompositions of calculated ^{7}Be wave functions by U(3) (left) and Sp$(3,\mathbb{R})$ (right) contributions, for the $\omega S = 0(3,0)1/2$ ground state band member $3/2^-_1$ (bottom), the $\omega S = 2(5,0)1/2$ excited band member $7/2^-_3$ (middle), and the strongly connected $11/2^-_1$ (top). Contributions are arranged by $N_{\rm ex}(\lambda,\mu)S$ and shown through $N_{\rm ex} = 2$.

However, these $9/2^-$ and $11/2^-$ states also have enhanced transitions to a particular high-lying $5/2^-$ state and $7/2^-$ state, well off the yrast line. Tracing $E2$ strengths to lower J reveals that these $5/2^-$ and $7/2^-$ states belong to an excited $K = 1/2$ rotational band [Fig. 2(a), upper dashed line]. One might therefore suspect the $9/2^-$ and $11/2^-$ states belong to the excited rotational band, albeit with energies below those expected for this band [Fig. 2(a), upper dotted line].

Returning to the Sp$(3,\mathbb{R}) \supset$ U(3) decompositions of Fig. 3 for insight, the wave functions of the ground state band members are dominated by a single U(3) irrep, namely, $\omega S = 0(3,0)1/2$, as expected (above) from a dynamical symmetry picture. About 60–70% of the probability (or norm) of these states comes from this U(3) irrep, as illustrated for the ground state [Fig. 3(e)], with the exception of the $5/2^-$ band member, which lies in a close doublet and undergoes two-state mixing.

This $0\hbar\omega$ Elliott U(3) description of the ground state band is dressed by $2\hbar\omega$ and higher excitations. We see that excitations within the same Sp$(3,\mathbb{R})$ irrep account for much of the remaining probability. For the ground state [Fig. 3(f)], the $\sigma S = 0(3,0)1/2$ Sp$(3,\mathbb{R})$ irrep accounts for over 80% of the probability, which comes from, e.g., the $\omega S = 2(5,0)1/2$ and $2(1,2)1/2$ irreps within this Sp$(3,\mathbb{R})$ irrep [recall Fig. 1(b)].

For the excited band, the largest U(3) contribution comes from $\omega S = 2(5,0)1/2$, e.g., ~40% for the $7/2^-$ band member [Fig. 3(c)]. This again suggests an Elliott rotational description, but now in the $2\hbar\omega$ space rather than in the traditional $0\hbar\omega$ shell model valence space. The U(3) symmetry is more diluted than for the ground state band, and dressing with higher excitations is again significant.

Moreover, we see that the excited band members lie almost entirely within the same $\sigma S = 0(3,0)1/2$ Sp$(3,\mathbb{R})$ irrep as the ground state band, e.g., ~70% for the $7/2^-$ band member [Fig. 3(d)]. While there are 8 different U(3) irreps with quantum numbers $\omega S = 2(5,0)1/2$ for ^{7}Be, the $2(5,0)1/2$ probability found in the calculated wave function arises almost entirely from the one such U(3) irrep lying in the $\sigma S = 0(3,0)1/2$ symplectic irrep.

Thus, the wave functions are consistent with an approximate Sp$(3,\mathbb{R}) \supset$ U(3) dynamical symmetry (Fig. 1). Indeed, the Sp$(3,\mathbb{R})$ symmetry is significantly better preserved than the U(3) symmetry.

Turning to the $9/2^-$ and $11/2^-$ states with strong transitions to both bands, these have predominantly $\omega S = 2(5,0)1/2$ U(3) content [Fig. 3(a)], like the excited band members but purer (~50%–60%). They likewise lie almost entirely within the ground state's $\sigma S = 0(3,0)1/2$ Sp$(3,\mathbb{R})$ irrep [Fig. 3(b)].

Thus, Sp$(3,\mathbb{R}) \supset$ U(3) dynamical symmetry provides a context for understanding both the emergent rotational features and the incomplete description provided for these features by a simple adiabatic rotational picture. Qualitatively, a $0\hbar\omega$ ground state band [$\omega S = 0(3,0)1/2$] and $2\hbar\omega$ excited band [$\omega S = 2(5,0)1/2$] lie within the same symplectic irrep [$\sigma S = 0(3,0)1/2$]. In a pure Elliott U(3) rotational description, the $9/2^-$ and $11/2^-$ states would simply be part of the excited band. Enhanced transitions among these states are a consequence of dynamical symmetry [Fig. 1(d)], reflecting the role of the isoscalar $E2$ operator as a generator connecting states with $\Delta N = \pm 2$ within an Sp$(3,\mathbb{R})$ irrep.

Yet, mixing of U(3) irreps within the Sp$(3,\mathbb{R})$ irrep, which becomes significant for the off-yrast excited band members ($J \leq 7/2$), manifests in deviations from a pure Elliott rotational picture. This breakdown is reflected in weaker in-band and interband $E2$ transitions involving the low-J excited band members [Fig. 2(a)], compared to the dynamical symmetry predictions [Fig. 1(d)], as well as the discontinuity in energies between the low-J and high-J members of this band.

For the remaining low-lying states in Fig. 2(a), the overall pattern of the spectrum is again qualitatively described by Sp$(3,\mathbb{R}) \supset$ U(3) dynamical symmetry. In Fig. 2(b), the symbols identify the largest Sp$(3,\mathbb{R})$ component, while dashed lines (where practical) connect states sharing the same largest U(3) component.

For many of the states near the yrast line the largest U(3) and Sp$(3,\mathbb{R})$ components contribute the preponderance of the probability. However, as we move to higher energy and away from the yrast line, contributions from other U(3) and Sp$(3,\mathbb{R})$ components become increasingly important (see Supplemental Material [72]). Furthermore, recall that, when two states are nearly degenerate in energy, they may undergo two-state mixing [brackets in Fig. 2(b)]. This serves both to mix the dynamical symmetry content and lift the energy degeneracy through level repulsion [3,74].

The dynamical symmetry picture accounts for the full set of states in the calculated low-lying ($0\hbar\omega$) spectrum and the overall pattern of their energies. In comparing Fig. 1(a) with Fig. 2(b), it is helpful to focus on the "constellations" formed when the calculated states are classified by their predominant $\mathrm{Sp}(3,\mathbb{R}) \supset \mathrm{U}(3)$ contributions. For instance, the calculated states [Fig. 2(b)] with largest component $\omega S = 0(1,1)3/2$ form a roughly trapezoidal constellation (up triangles), while those with $\omega S = 0(1,1)1/2$ form two nearly degenerate diamond-shaped constellations (down triangles), as in the dynamical symmetry picture [Fig. 1(a)]. Counterparts to the expected higher-lying $\omega S = 0(0,0)3/2$ (hexagon) and $\omega S = 0(0,0)1/2$ (circle) are also found.

The relationship between the calculated spectrum and the dynamical symmetry picture, shown here for the Daejeon16 interaction, is robust across choice of internucleon interaction. This is illustrated for, e.g., the JISP16 [75] and Entem-Machleidt $\mathrm{N^3LO}$ chiral perturbation theory [76] interactions in the Supplemental Material [72].

Conclusion.—We have seen that $\mathrm{Sp}(3,\mathbb{R}) \supset \mathrm{U}(3)$ dynamical symmetry, as laid out in Fig. 1, provides an organizing scheme for understanding the entire low-lying *ab initio* calculated spectrum of ^{7}Be, as shown in Fig. 2. Symmetry is reflected not merely in the decompositions of the individual wave functions (Fig. 3), but in the overall arrangement of energies, which is remarkably consistent with a simple dynamical symmetry Hamiltonian (2), and in the $E2$ transition patterns among them.

Essential features of the dynamical symmetry structure are a $0\hbar\omega$ spectrum well-described in an Elliott U(3) picture, but dressed by $2\hbar\omega$ and higher contributions from within the $\mathrm{Sp}(3,\mathbb{R})$ irrep, and excited states reflecting $2\hbar\omega$ excitations within the $\mathrm{Sp}(3,\mathbb{R})$ irrep, related to the lower-lying states by strong quadrupole transitions. Although the purity of U(3) symmetry falls off away from the yrast line, as reflected in the inability of a simple rotational description to simultaneously describe both the low-J members of the excited band and the strongly connected $9/2^-$ and $11/2^-$ states, the persistence of $\mathrm{Sp}(3,\mathbb{R})$ symmetry explains the presence of these strong transitions.

The connection between the ground state and excited bands by the symplectic raising operators, which physically represent creation operators for the giant monopole and quadrupole resonances, is suggestive of the emergence of collective vibrational degrees of freedom. In the light, weakly bound ^{7}Be system, such an interpretation can at most be approximate. In the present bound state formalism, it moreover remains uncertain how the structure of the calculated excited band relates to the structure of physical resonances [19].

Nonetheless, the presence of rotational bands with strong $E2$ connections may be taken as a possible precursor to rotational-vibrational structure in heavier and more strongly bound systems. Indeed, the emergence of $\mathrm{Sp}(3,\mathbb{R})$ symmetry as an organizing scheme for nuclear structure in light nuclei provides a link to more purely collective interpretations of the dynamics through the rotation-vibration degrees of freedom which naturally arise in the classical (large quantum number) limit of the symplectic description [36,45,77–79].

We thank David J. Rowe for indispensable assistance with the $\mathrm{Sp}(3,\mathbb{R})$ formalism, Calvin W. Johnson, James P. Vary, and Pieter Maris for valuable discussions, and Nadya A. Smirnova and Jakub Herko for comments on the manuscript. This material is based upon work supported by the U.S. Department of Energy, Office of Science, Office of Nuclear Physics, under Award No. DE-FG02-95ER-40934, by the U.S. Department of Energy, Office of Science, Office of Workforce Development for Teachers and Scientists, Graduate Student Research (SCGSR) program, under Contract No. DE-AC05-06OR23100, and by the Research Corporation for Science Advancement, under a Cottrell Scholar Award. TRIUMF receives federal funding via a contribution agreement with the National Research Council of Canada. This research used computational resources of the University of Notre Dame Center for Research Computing and of the National Energy Research Scientific Computing Center (NERSC), a U.S. Department of Energy, Office of Science, user facility supported under Contract No. DE-AC02-05CH11231.

[1] P. Ring and P. Schuck, *The Nuclear Many-Body Problem* (Springer-Verlag, New York, 1980).
[2] I. Talmi, *Simple Models of Complex Nuclei: The Shell Model and Interacting Boson Model*, Contemporary Concepts in Physics Vol. 7 (Harwood Academic Publishers, Chur, Switzerland, 1993).
[3] R. F. Casten, *Nuclear Structure from a Simple Perspective*, 2nd ed. (Oxford University Press, Oxford, New York, 2000), Vol. 23.
[4] D. J. Rowe and J. L. Wood, *Fundamentals of Nuclear Models: Foundational Models* (World Scientific, Singapore, 2010).
[5] P. Navrátil, J. P. Vary, and B. R. Barrett, Phys. Rev. Lett. **84**, 5728 (2000).
[6] G. Hagen, D. J. Dean, M. Hjorth-Jensen, T. Papenbrock, and A. Schwenk, Phys. Rev. C **76**, 044305 (2007).
[7] S. Quaglioni and P. Navrátil, Phys. Rev. C **79**, 044606 (2009).
[8] S. Bacca, N. Barnea, and A. Schwenk, Phys. Rev. C **86**, 034321 (2012).
[9] T. Dytrych, K. D. Launey, J. P. Draayer, P. Maris, J. P. Vary, E. Saule, U. Catalyurek, M. Sosonkina, D. Langr, and M. A. Caprio, Phys. Rev. Lett. **111**, 252501 (2013).
[10] S. Baroni, P. Navrátil, and S. Quaglioni, Phys. Rev. C **87**, 034326 (2013).
[11] J. Carlson, S. Gandolfi, F. Pederiva, S. C. Pieper, R. Schiavilla, K. E. Schmidt, and R. B. Wiringa, Rev. Mod. Phys. **87**, 1067 (2015).
[12] S. R. Stroberg, H. Hergert, J. D. Holt, S. K. Bogner, and A. Schwenk, Phys. Rev. C **93**, 051301(R) (2016).

[13] S. L. Henderson, T. Ahn, M. A. Caprio, P. J. Fasano, A. Simon, W. Tan, P. O'Malley, J. Allen, D. W. Bardayan, D. Blankstein, B. Frentz, M. R. Hall, J. J. Kolata, A. E. McCoy, S. Moylan, C. S. Reingold, S. Y. Strauss, and R. O. Torres-Isea, Phys. Rev. C **99**, 064320 (2019).
[14] T. Neff and H. Feldmeier, Nucl. Phys. **A738**, 357 (2004).
[15] S. C. Pieper, R. B. Wiringa, and J. Carlson, Phys. Rev. C **70**, 054325 (2004).
[16] P. Maris, J. Phys. Conf. Ser. **402**, 012031 (2012).
[17] T. Yoshida, N. Shimizu, T. Abe, and T. Otsuka, Few-Body Syst. **54**, 1465 (2013).
[18] P. Navrátil, S. Quaglioni, G. Hupin, C. Romero-Redondo, and A. Calci, Phys. Scr. **91**, 053002 (2016).
[19] M. Vorabbi, P. Navrátil, S. Quaglioni, and G. Hupin, Phys. Rev. C **100**, 024304 (2019).
[20] M. A. Caprio, P. Maris, and J. P. Vary, Phys. Lett. B **719**, 179 (2013).
[21] P. Maris, M. A. Caprio, and J. P. Vary, Phys. Rev. C **91**, 014310 (2015); P. Maris, M. A. Caprio, and J. P. Vary, Phys. Rev. C **99**, 029902(E) (2019).
[22] M. A. Caprio, P. Maris, J. P. Vary, and R. Smith, Int. J. Mod. Phys. **24**, 1541002 (2010).
[23] G. R. Jansen, M. D. Schuster, A. Signoracci, G. Hagen, and P. Navrátil, Phys. Rev. C **94**, 011301(R) (2016).
[24] M. Gell-Mann, Phys. Rev. **125**, 1067 (1962).
[25] B. G. Wybourne, *Classical Groups for Physicists* (Wiley, New York, 1974).
[26] A. O. Barut and R. Raczka, *Theory of Group Representations and Applications* (Polish Scientific Publishers, Warsaw, 1977).
[27] F. Iachello, in *Lie Algebras, Cohomology, and New Applications to Quantum Mechanics*, Contemp. Math. Vol. 160, edited by N. Kamran and P. Olver (American Mathematical Society, Providence, Rhode Island, 1994), p. 151.
[28] F. Iachello, *Lie Algebras and Applications*, 2nd ed., Lecture Notes in Physics Vol. 891 (Springer, Berlin, 2015).
[29] A. Arima and F. Iachello, Phys. Rev. Lett. **35**, 1069 (1975).
[30] A. Arima and F. Iachello, Ann. Phys. (N.Y.) **99**, 253 (1976); **111**, 201 (1978); O. Scholten, F. Iachello, and A. Arima, Ann. Phys. (N.Y.) **115**, 325 (1978); A. Arima and F. Iachello, Ann. Phys. (N.Y.) **123**, 468 (1979).
[31] J. P. Elliott, Proc. R. Soc. A **245**, 128 (1958); **245**, 562 (1958); J. P. Elliott and M. Harvey, Proc. R. Soc. A **272**, 557 (1963); J. P. Elliott and C. E. Wilsdon, Proc. R. Soc. A **302**, 509 (1968).
[32] M. Harvey, Adv. Nucl. Phys. **1**, 67 (1968).
[33] K. T. Hecht, Annu. Rev. Nucl. Sci. **23**, 123 (1973).
[34] G. Rosensteel and D. J. Rowe, Phys. Rev. Lett. **38**, 10 (1977).
[35] G. Rosensteel and D. J. Rowe, Ann. Phys. (N.Y.) **126**, 343 (1980).
[36] D. J. Rowe, Rep. Prog. Phys. **48**, 1419 (1985).
[37] D. J. Rowe, Prog. Part. Nucl. Phys. **37**, 265 (1996).
[38] J. Carvalho, P. Park, and D. J. Rowe, Phys. Lett. **119B**, 249 (1982).
[39] P. Park, J. Carvalho, M. Vassanji, and D. J. Rowe, Nucl. Phys. **A414**, 93 (1984).
[40] J. P. Draayer, K. J. Weeks, and G. Rosensteel, Nucl. Phys. **A413**, 215 (1984).
[41] G. Rosensteel, J. P. Draayer, and K. J. Weeks, Nucl. Phys. **A419**, 1 (1984).
[42] J. Escher and J. P. Draayer, J. Math. Phys. (N.Y.) **39**, 5123 (1998).
[43] J. Escher and A. Leviatan, Phys. Rev. Lett. **84**, 1866 (2000).
[44] J. Escher and A. Leviatan, Phys. Rev. C **65**, 054309 (2002).
[45] D. J. Rowe, A. E. McCoy, and M. A. Caprio, Phys. Scr. **91**, 033003 (2016); **91**, 049601 (2016).
[46] D. J. Rowe, Phys. Rev. C **101**, 054301 (2020).
[47] T. Dytrych, K. D. Sviratcheva, C. Bahri, J. P. Draayer, and J. P. Vary, Phys. Rev. Lett. **98**, 162503 (2007).
[48] T. Dytrych, K. D. Sviratcheva, C. Bahri, J. P. Draayer, and J. P. Vary, J. Phys. G **35**, 095101 (2008).
[49] T. Dytrych, K. D. Sviratcheva, J. P. Draayer, C. Bahri, and J. P. Vary, J. Phys. G **35**, 123101 (2008).
[50] J. P. Draayer, T. Dytrych, K. D. Launey, and D. Langr, Prog. Part. Nucl. Phys. **67**, 516 (2012).
[51] T. Dytrych, A. C. Hayes, K. D. Launey, J. P. Draayer, P. Maris, J. P. Vary, D. Langr, and T. Oberhuber, Phys. Rev. C **91**, 024326 (2015).
[52] T. Dytrych, P. Maris, K. D. Launey, J. P. Draayer, J. P. Vary, D. Langr, E. Saule, M. A. Caprio, U. Catalyurek, and M. Sosonkina, Comput. Phys. Commun. **207**, 202 (2016).
[53] K. D. Launey, T. Dytrych, and J. P. Draayer, Prog. Part. Nucl. Phys. **89**, 101 (2016).
[54] T. Dytrych, K. D. Launey, J. P. Draayer, D. J. Rowe, J. L. Wood, G. Rosensteel, C. Bahri, D. Langr, and R. B. Baker, Phys. Rev. Lett. **124**, 042501 (2020).
[55] A. E. McCoy, M. A. Caprio, and T. Dytrych, Ann. Acad. Rom. Sci. Ser. Chem. Phys. Sci. **3**, 17 (2018), http://www.aos.ro/wp-content/anale/PCVol3Nr1Art.2.pdf.
[56] A. E. McCoy, *Ab initio* multi-irrep symplectic no-core configuration interaction calculations, Ph.D. thesis, University of Notre Dame, 2018.
[57] O. Castanos, J. P. Draayer, and Y. Leschber, Z. Phys. A **329**, 33 (1988).
[58] D. R. Tilley, C. M. Cheves, J. L. Godwin, G. M. Hale, H. M. Hofmann, J. H. Kelley, C. G. Sheu, and H. R. Weller, Nucl. Phys. **A708**, 3 (2002).
[59] M. Hamermesh, *Group Theory and Its Applications to Physical Problems* (Dover Publications, Inc., Reading, 1962).
[60] J. P. Draayer, Y. Leschber, S. C. Park, and R. Lopez, Comput. Phys. Commun. **56**, 279 (1989).
[61] D. R. Inglis, Rev. Mod. Phys. **25**, 390 (1953).
[62] G. Rosensteel, J. Math. Phys. (N.Y.) **21**, 924 (1980).
[63] D. J. Rowe, G. Rosensteel, and R. Carr, J. Phys. A **17**, L399 (1984).
[64] E. J. Reske, $\mathrm{Sp}(6,R)$ symmetry and the giant quadrupole resonance in ^{24}Mg, Ph.D. Thesis, University of Michigan, 1984.
[65] Y. Suzuki and K. T. Hecht, Nucl. Phys. **A455**, 315 (1986).
[66] Y. Suzuki, Nucl. Phys. **A448**, 395 (1986).
[67] A. M. Shirokov, I. J. Shin, Y. Kim, M. Sosonkina, P. Maris, and J. P. Vary, Phys. Lett. B **761**, 87 (2016).
[68] F. Q. Luo, M. A. Caprio, and T. Dytrych, Nucl. Phys. **A897**, 109 (2013).

[69] M. A. Caprio, A. E. McCoy, and P. J. Fasano, J. Phys. G (2020), https://doi.org/10.1088/1361-6471/ab9d38.
[70] B. R. Barrett, P. Navrátil, and J. P. Vary, Prog. Part. Nucl. Phys. **69**, 131 (2013).
[71] J. Suhonen, *From Nucleons to Nucleus: Concepts of Microscopic Nuclear Theory* (Springer-Verlag, Berlin, 2007).
[72] See Supplemental Material at http://link.aps.org/supplemental/10.1103/PhysRevLett.125.102505 for U(3) and Sp$(3,\mathbb{R})$ decompositions of calculated eigenstates.
[73] M. A. Caprio, P. J. Fasano, P. Maris, A. E. McCoy, and J. P. Vary, Eur. Phys. J. A **56**, 120 (2020).
[74] K. Heyde and J. L. Wood, *Quantum Mechanics for Nuclear Structure* (IOP Publishing, Bristol, UK, 2020), Vol. 1.
[75] A. M. Shirokov, J. P. Vary, A. I. Mazur, and T. A. Weber, Phys. Lett. B **644**, 33 (2007).
[76] D. R. Entem and R. Machleidt, Phys. Rev. C **68**, 041001(R) (2003).
[77] R. Le Blanc, J. Carvalho, and D. J. Rowe, Phys. Lett. **140B**, 155 (1984).
[78] D. J. Rowe and M. G. Vassanji, Nucl. Phys. **A504**, 76 (1989).
[79] R. Le Blanc, J. Carvalho, M. Vassanji, and D. J. Rowe, Nucl. Phys. **A452**, 263 (1986).